Journal of Petroleum Exploration and Production Technology (2019) 9:17–29
https://doi.org/10.1007/s13202-018-0471-2

ORIGINAL PAPER - EXPLORATION GEOLOGY

Occurrence characteristics and main controlling factors of movable fluids in Chang 8_1 reservoir, Maling Oilfield, Ordos Basin, China

Pan Li[1,2] · Wei Sun[1,2] · Bolin Wu[1,2] · Rui Huang[3] · Yongli Gao[4] · Jian Yan[4] · Hexin Huang[1,2]

Received: 24 December 2017 / Accepted: 4 April 2018 / Published online: 13 July 2018

Abstract

The Chang 8_1 reservoir in the Maling Oilfield, Ordos Basin, China, is featured by complex microscopic pore structure and obviously different fluid distribution characteristics. It is a typical low-porosity and low-permeability reservoir. To analyze the occurrence characteristics and main controlling factors of movable fluids in Chang 8_1 reservoir, this study carries out NMR-based quantitative analysis, which is combined with several microscopic experiments involving analyses of conventional physical properties, image granularity, casting thin sections and electron microscope scanning. There are mainly three types of T_2 spectrum curves in terms of the shape, namely left-high-peak–right-low-peak, left-low-peak–right-high-peak, and unimodal shapes. Permeability is well correlated with movable fluid saturation, and larger physical property variation results in more significant movable fluid saturation variation. The main controlling factors that contribute to the obviously different occurrence characteristics of movable fluids are demonstrated to be pore type, pore–throat radius, pore–throat radius ratio, sorting coefficient, effective pore–throat volume, and clay mineral filling. Among them, pore and throat radii and pore–throat radius ratio are more dominant factors, followed by effective pore–throat volume and sorting coefficient. The clay mineral filling, pore type and physical property have the least influence on the movable fluid saturation.

Keywords Maling Oilfield · Chang 8_1 reservoir · Occurrence characteristics of movable fluids · Nuclear magnetic resonance · Microscopic pore structure characteristics

Introduction

Movable fluid saturation, referring to a critical saturation value measured by nuclear magnetic resonance (NMR) experiments, can royally reflect occurrence characteristics of fluids in the pore structure (Gao et al. 2015; Yang et al. 2013; Zhang et al. 2015). In this context, the reservoir pore structure can be intuitively and quickly evaluated by measuring the movable fluid saturation, which can help effectively evaluate the development effect in the low-permeability sandstone reservoirs. The NMR-based measurement can provide important information about movable fluid saturation, based on which further works can be done to characterize the microscopic pore structure and analyze variation characteristics and differences of movable fluids in the reservoir.

In the past decades, lots of works have been done in the NMR logging field (Al-Mahrooqi et al. 2006; Dlubac et al. 2013). In the early 1990s, NUMAR Company successfully developed its first pulse NMR instrument, and acquired, for the first time, the T_2 relaxation spectrum reflecting relaxation characteristics of rocks based on the NMR multi-index inversion algorithm (Cai et al. 2013; Li et al. 2008; Zou et al. 2012). In 1991, Langfang Branch of Research Institute of Petroleum Exploration and Development of PetroChina introduced the first world-class superconducting NMR imager and carried out a large number of analyses concerning reservoir physical properties; then in 1996, it successfully developed a comprehensive NMR rock sample analysis system, which was able to accurately measure porosity, permeability, movable fluid saturation and oil saturation; subsequently, basic research and calibration works were done, such as determination of T_2 cut-off

✉ Pan Li
122078558@qq.com

1 State Key Laboratory of Continental Dynamics of Ministry of Geology, Northwest University, Xi'an 710069, China

2 Department of Geology, Northwest University, Xi'an 710069, China

3 CNPC, Richfit Information Technology Co. Ltd, Beijing 100000, China

4 College of Petroleum Engineering, Xi'an Shiyou University, Xi'an 710065, China

values of movable fluids in various kinds of rocks as well as establishment of NMR-porosity and NMR-permeability interpretation models (Freeman and Heaton 2000; Megawati et al. 2012; Nelson 2009; Zheng and Liu 2015). At present, NMR technology is mainly applied in two fields, namely the indoor rock sample analysis and the logging interpretation (Bai et al. 2016; Zhou et al. 2016). The former application can reflect NMR response characteristics, NMR porosity and NMR permeability of different types of reservoirs (Cao et al. 2016). It can be combined with centrifugal experiments to calibrate T_2 cut-off value of movable fluids, while it can also be combined with displacement experiments to study oil–water and gas–water seepage mechanisms (Ren et al. 2015). The latter application can precisely provide information about reservoir physical properties, including effective porosity, permeability, bound water saturation, and pore size distribution, according to the resonance signals generated by the hydrogen atoms in the reservoir fluid in the magnetic field. Further, movable and bound fluid volumes can be, respectively, calculated, which are critical and reliable parameters for pore structure analysis (Chen et al. 2015; Liu et al. 2016; Ma et al. 2012; Zhao et al. 2016). In the evaluation of low-permeability tight sandstone reservoirs, not only the conventional parameters (e.g. reservoir thickness, continuity, distribution, porosity and permeability) but also the movable fluid properties should be highlighted.

Chang 8_1 reservoir in the Maling Oilfield, Ordos Basin, is featured by complex microscopic pore structure, low movable fluid saturation and diversified fluid distribution pattern. Previous works paid more attention to the measurement of movable fluid parameters (still not accurate enough), whereas investigations of movable fluid occurrence characteristics and controlling factors of movable fluids were insufficient. To more accurately characterize reservoir quality with fluid saturation parameters, this study conducts NMR measurements to quantitatively analyze the occurrence characteristics of movable fluids in the Chang 8_1 reservoir, which are combined with several microscopic experiments to explore the main controlling factors of diversified fluid occurrence characteristics. Results of this study can provide certain scientific basis for potential oil recovery enhancement in the Oilfield.

Geological setting and experiment

Geological background and samples

Geographically located in the Longdong Area of Gansu Province, China, and tectonically situated in the north Shaanxi slope structure zone of Ordos Basin, Maling Oilfield is known as the main oil and gas exploration and development area of Changqing Oilfield of Petro China due to its abundant reserves and large area (Ren et al. 2015a, b). This study targets the Chang 8_1 reservoir of Triassic Yanchang Formation (Fig. 1). During its depositional period, Maling Oilfield was controlled by the provenance from the northeast, southwest and west as well as the sedimentary system in the southwest. Delta front deposits were dominant.

According to the thin section observation and detrital component statistical analysis, Chang 8_1 reservoir mainly consists of lithic feldspathic sandstone and feldspathic lithic sandstone. Pore types are mainly micropores and dissolved intergranular pores, with porosity ranging from 6.78 to 12.07% (average 10.55%) and permeability ranging from 0.28×10^{-3} to 2.301×10^{-3} μm^2 (average 0.97×10^{-3} μm^2).

As a typical low-porosity and low-permeability reservoir, Chang 8_1 reservoir is characterized by small pores and throats, poor connectivity between pores and throats, complex pore and throat types, and various seepage influencing factors. Accordingly, this study adopts a variety of microscopic experiments to quantitatively characterize the occurrence characteristics of movable fluids, including conventional physical property analysis (193 samples), casting thin section observation (39 samples) and scanning electron microscopy (SEM) analysis (24 samples).

Based on the high-speed centrifugal experiments with different centrifugal forces on 13 core samples, T_2 spectra of simulated formation water-saturated core samples are obtained. Then, according to the T_2 spectrum shapes and corresponding centrifugal forces, it is found that the critical relaxation time value between bound fluids and movable fluids is 13.895 ms (Ren et al. 2016) (Table 1). To clarify variation characteristics of movable fluids in different experimental samples, T_2 values are divided into three intervals (<10, 10–100, and >100 ms) in this study. According to the standards of Chinese Oil and Gas Industry, the reservoirs are classified into Class I (excellent), Class II (good), Class III (average), Class IV (fair) and Class V (poor). This study classifies the reservoir into five classes according to the movable fluid saturation, which, respectively, correspond to the range of >65, 50–65, 35–50, 20–35, and <20% (Huang et al. 2016; Ren et al. 2016a, b).

Experimental methods and procedures

NMR experiments

Nuclear magnetic resonance experiments can characterize the occurrence state of movable fluids, with relaxation time as an important indicator. Generally, relaxation time is not only influenced by physical properties of rocks but also the characteristics of fluids (Dai et al. 2016; Qu et al. 2016). Relaxation time can be used to characterize the occurrence state of movable fluids, while different T_2 spectra correspond to different pore–throat structures of different types of rocks. For the water-saturated cores, free water in them has larger T_2 value, indication bigger pores, while bound water has

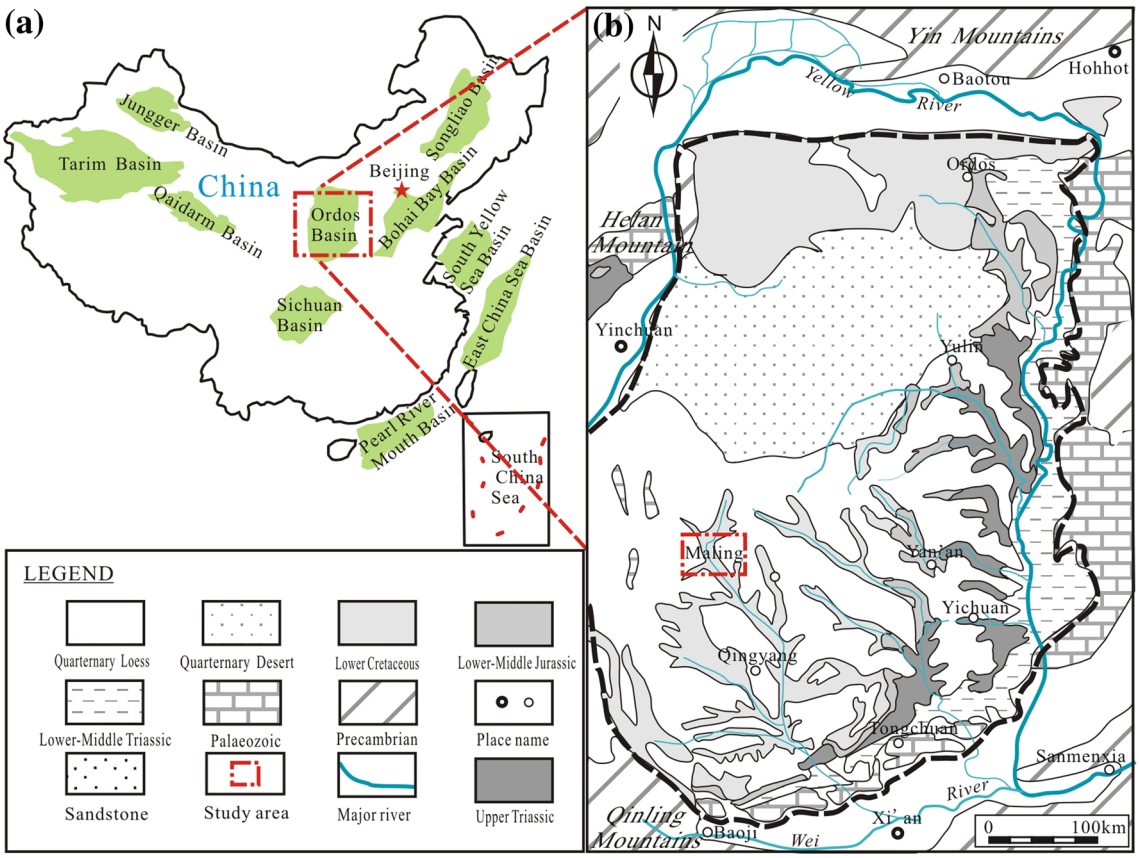

Fig. 1 Geographic location of Maling Oilfield (**b**) in the Ordos Basin (**a**)

Table 1 Physical property parameters of Chang 8_1 reservoir

Sample ID	Well ID	Porosity (%)	Permeability (10^{-3} μm^2)	Movable fluid saturation (%)	Movable fluid porosity (%)	T_2 spectral interval (%)			Classification
						< 10 ms	10–100 ms	> 100 ms	
1	H23	12.07	2.30	80.59	9.73	37.36	45.75	16.89	I
2	H56	9.08	0.31	38.15	3.46	77.48	22.52	0.00	III
3	L78	11.59	0.69	30.97	3.59	92.71	6.60	0.69	IV
4	L275-21	10.08	0.28	34.92	3.52	80.45	13.49	6.06	IV
5	L91	11.96	2.12	61.74	5.58	18.61	70.41	10.99	II
6	L98	11.78	1.37	53.16	6.26	73.31	22.04	4.65	II
7	L126	10.32	0.88	31.70	3.27	63.75	26.72	9.53	IV
8	M21	9.00	0.33	18.85	1.70	62.11	29.70	8.19	V
9	M23	6.78	0.9	44.19	3.00	79.69	18.78	1.53	III
10	M30	10.31	0.43	33.32	3.44	92.71	6.70	0.59	IV
11	M31	10.70	0.51	47.28	5.06	77.83	19.77	2.40	III
12	Y285	11.87	1.49	49.87	5.92	77.48	20.52	2.00	III
13	B285	11.54	0.99	52.98	6.11	75.34	24.60	0.06	II
Max		12.07	2.30	80.59	9.73	92.71	70.41	16.89	–
Mean		10.32	0.83	44.44	4.66	69.91	25.20	6.31	–
Min		6.78	0.09	18.85	1.28	18.61	6.60	0.00	–
Contrast		1.78	25.57	4.28	7.61	4.98	10.66	–	–

smaller T_2 value, indicating small pores and immovable fluids (Gao et al. 2015; Wang et al. 2017).

According to the industry standard (SY/T6490-2000), MagneT2000 instrument is used for NMR experiments. A total of 13 samples are conducted with centrifugal experiments under the empirically ideal centrifugal pressure of 300 Psi (about 2.07 MPa). Based on integration of the results and the empirical value in the study area, 13.895 ms is adopted as the boundary between movable and bound fluids (Table 1; Fig. 2).

Casting thin section and SEM observations

In this study, casting thin sections with the thickness of 0.03 mm and the area no less than 15 mm × 15 mm are observed under Leica DMRXHC and Linkam THMSG600 optical microscopes in the State Key Laboratory of Continental Dynamics of Northwestern University of China. Through the observation of 39 thin sections, information about surface porosity, pore and throat radii, pore–throat coordination number, and lithic composition is obtained. Meanwhile, using the FEI Quanta 650FEG device in the State Key Laboratory of Continental Dynamics of Northwestern University of China, SEM observation can help analyze the pore–throat property and clay mineral occurrence in the 24 samples, which can more accurately reflect the micro changes of mineral rocks (Fig. 4).

NMR-based movable fluid characterization

When irradiating the hydrogen nuclei in the fluid medium with different resonance frequencies in the static magnetic field, electromagnetic waves with the corresponding frequency will be absorbed and polarized, referred to as nuclear magnetic resonance (Wu et al. 2017; Yao and Liu 2012; Zhao et al. 2017). This is the principle of movable fluid saturation measurement in the cores. According to Boltzmann's law, the ratio between the low-level and the excited-state magnetic nuclei remains roughly the same. The excited-state high-level magnetic nuclei undergo energy reduction and transit to low-level magnetic nuclei. Such non-radiative process is referred to as relaxation. In practice, when the radio-frequency field is removed, the amplitude variations of the NMR signals in the hydrogen nuclei can be measured (Daigle and Johnson 2016; Li et al. 2008). The signal amplitude decreases exponentially with time until disappearing,

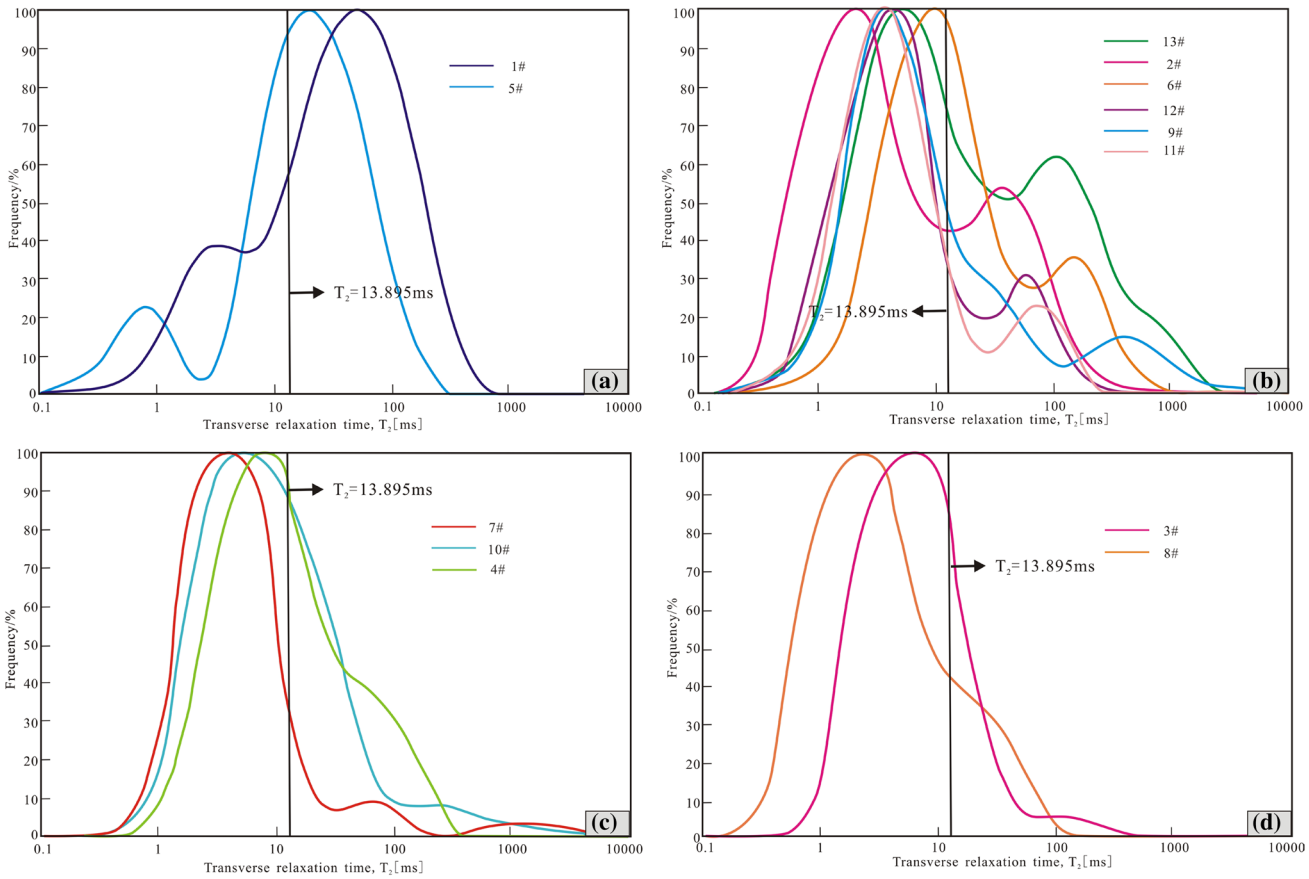

Fig. 2 T_2 spectra of Chang 8_1 reservoir in the Maling Oilfield

and corresponding attenuation time is referred to as the relaxation time, which can be divided into longitudinal relaxation time (T_1) and transverse relaxation time (T_2). Since transverse relaxation corresponds to the transition of energy from protons to rock particle surface, it can be used to describe the signal attenuation rate (Ren et al. 2017; Shi et al. 2016; Zheng et al. 2013).

Nuclear magnetic resonance experiments can provide much original information, such as physical properties, pore–throat distribution and size, reservoir space, and fluid type, which contributes to the T_2 spectra through their fitting and transformation. T_2 is positively correlated to the pore diameter, and also reflects the specific surface area of the rock pores. The precondition is that the core should be fully water saturated. The T_2 cutoff value corresponds to the upper size limit of pores with bound fluids (Yan et al. 2017; Yao et al. 2013).

Under certain centrifugal test conditions, the NMR signals produced during the excitation of nuclei in fluids with different states in the pores of water-saturated cores are observed. Then, T_2 distribution patterns are compared and analyzed, which can help identify the properties of fluids on the rock pore surface as well as certain geological information including physical property, pore–throat structure, movable fluid volume, effective porosity, and upper limit of reservoir charging. Therefore, relevant works can promote the reasonable assessment of reservoir development potential.

Results and discussion

T_2 spectrum distribution characteristics

Bound fluid is mainly, although not absolutely, distributed in the tiny pores, while movable fluid is primarily in the big pores. As Chang 8_1 reservoir is featured by small pore and throat size, complex pore–throat structure and uneven pore throat coordination number, many large pores and throats are blocked by small or isolated pores, resulting in the poor pore–throat connectivity. Under the action of centrifugal force, T_2 spectrum distribution is highly diversified, which leads to huge difference of movable fluid occurrence characteristics.

Nuclear magnetic resonance experiments show that movable fluid saturation values of 13 core samples range from 18.85 to 80.59% with an average of 42.06%. According to the abovementioned classification standard, Class III and Class IV reservoirs are dominant in the study area. There are mainly three types of T_2 spectrum shapes, namely left-high-peak–right-low-peak (samples 2, 6, 9, 11, 12, and 13), left-low-peak–right-high-peak (samples 1 and 5), and unimodal shapes (samples 3, 4, 7, 8, and 10) (Fig. 2) in the condition that the T_2 cutoff value for bound fluid is empirically set as 13.895 ms. As illustrated in Table 1, smaller T_2 value corresponding to the main peaks in the left-high-peak–right-low-peak spectrum indicates lower movable fluid saturation, while larger T_2 value corresponding to the main peaks in the left-low-peak–right-high-peak spectrum indicates lower movable fluid saturation.

Movable fluid occurrence characteristics and controlling factors

Influence of reservoir physical properties

As shown in Fig. 3, the correlation coefficient of movable fluid saturation and porosity is 0.2424, much smaller than that of movable fluid saturation and permeability, which is 0.7467. Therefore, it is safe to conclude that movable fluid saturation is more strongly correlated with permeability than porosity.

It is also found that the 13 samples have a wide range of movable fluid saturation, and the movable fluid saturation does not necessarily increase with porosity and permeability. For instance, among samples 4, 8, and 3, their permeability increases from 0.28×10^{-3} to 0.33×10^{-3} μm^2 and then 0.69×10^{-3} μm^2, while their movable fluid saturations are, respectively, 34.92, 18.85 and 30.97%. However, the overall trend is that the movable fluid saturation generally increases with permeability. Meanwhile, it can be also clearly seen that movable fluid porosity is more positively correlated with permeability than porosity, with respective correlation coefficients of 0.6582 and 0.5307. Overall, compared to movable fluid saturation, movable fluid porosity is more positively correlated with physical properties. In other words, movable fluid saturation is less influenced by the physical properties. Therefore, physical properties cannot completely reflect the occurrence characteristics of movable fluids, as they are not controlled by single-reservoir parameters.

Influence of pore types

Through observation of conventional and casting thin sections, it is found that there are various types of pores in the Chang 8_1 reservoir, with dominant intergranular pores and dissolved pores (Fig. 4a, b); there are a few unevenly distributed lithic dissolved pores and intercrystal pores; micro-fractures are not developed; and the surface porosity is low (Table 2). All these indicate great porosity loss due to the strong destruction of primary intergranular pores by mechanical compaction, cementation, and filling, and dissolution contributes little to the surface porosity.

It can be seen from Fig. 5 that there is a relatively good correlation between intergranular pore and dissolved pore volumes and movable fluid saturation, with the correlation

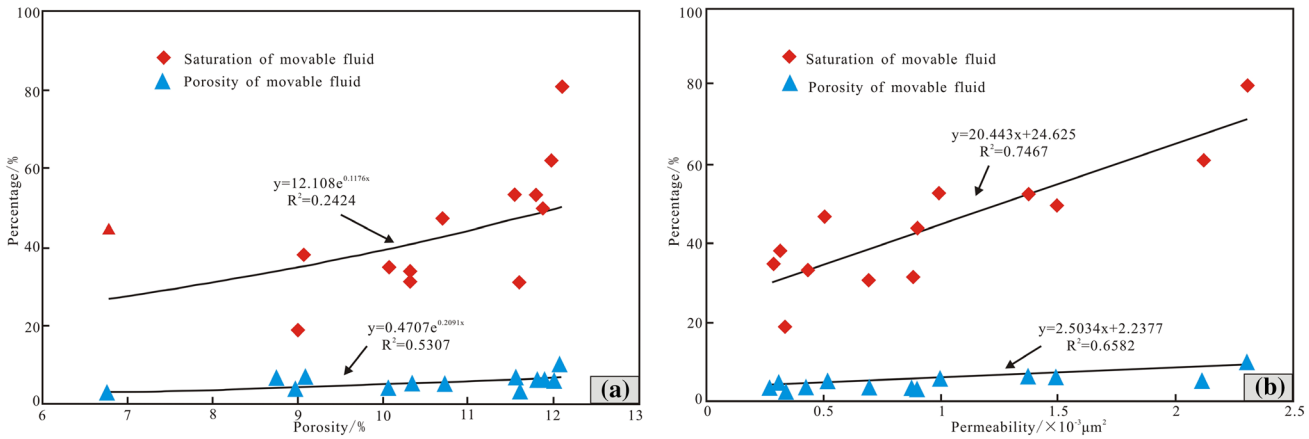

Fig. 3 Correlation of movable fluid parameters and physical properties of Chang 8_1 reservoir

coefficient reaching 0.7225. Meanwhile, surface porosity is also well correlated with movable fluid saturation with the correlation coefficient of 0.7169. In addition, intercrystal pores are found to be rarely correlated with movable fluid saturation with the correlation coefficient as low as 0.0954. It can be seen that more developed feldspar dissolution pores generally contribute to higher reservoir movable fluid saturation, and intercrystal pores in the cement fillings have small influence on movable fluid saturation. Moreover, surface porosity is demonstrated to be more correlated with movable fluid saturation than physical property, and all the surface porosity values are less than the corresponding porosity values.

Influence of microscopic pore structure characteristics

The main pore types in Chang 8_1 reservoir are residual intergranular pores and feldspar dissolved pores, while only those pores accessible to movable fluids are effective. This

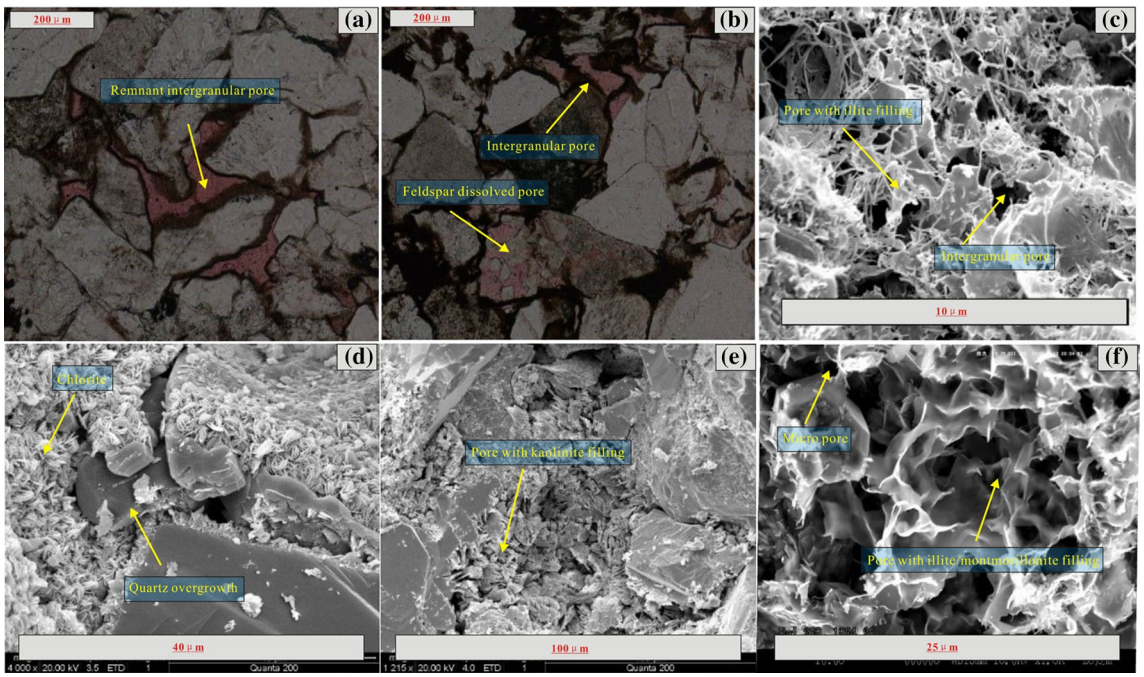

Fig. 4 Characteristics of pore structures and clay mineral contents in the casting thin sections and SEM sections. **a** Well L98, 2467.18 m, residual intergranular pore; **b** Well L126, 2163.94 m, feldspar dissolution pores; **c** Well H56, 2484.52 m, illite; **d** Well L78, 2181.1 m, chlorite film; **e** Well L91, 2396.9 m, kaolinite filling; **f** Well B455, 2026.24 m, illite/smectite mixed layer

Table 2 Relationship between pore parameters and movable fluid saturation in the Chang 8_1 reservoir

Sample ID	Well ID	Depth (m)	Quartz (%)	Feldspar (%)	Intergranular pore (%)	Dissolved pore (%)	Intergranular pore + dissolved pore (%)	Intercrystal pore (%)	Surface porosity (%)	Movable fluid saturation (%)
1	H23	2531.65	38.22	26.3	2.98	1.32	4.3	0.4	6.5	80.59
2	H56	2484.52	28.7	32.5	2.04	1.08	3.12	0.01	2.88	38.15
3	L78	2181.1	37.51	25.97	1.44	1.28	2.72	0.35	4.91	30.97
4	L275-21	2420.1	35.5	36	1.09	1.85	2.94	0.16	2.53	34.92
5	L91	2396.9	35	30.22	0.99	2.48	3.47	0.29	5.8	61.74
6	L98	2467.18	36.5	35	3.39	0.9	4.29	0.31	5.65	53.16
7	L126	2163.94	30	23.76	1.89	0.7	2.59	0.19	2.14	31.7
8	M21	2483.35	34	34.33	0.53	1.43	1.96	0.34	1.6	18.85
9	M23	2437.7	34.43	28.8	0.51	2.72	3.23	0	3	44.19
10	M30	2661.2	36	34.5	2.18	0.6	2.78	0.12	2.37	33.32
11	M31	2439.3	40.2	24	2.18	1.8	3.98	0.15	3.9	47.28
12	Y285	2293.6	37	31.09	3.03	1	4.03	0.24	4.67	49.87
13	B455	2026.24	35.19	30.72	2.33	1.84	4.17	0.27	5.49	52.98

study carries out high-pressure and constant-pressure mercury intrusion tests on 13 samples to quantify the volume and heterogeneity parameters of pore space in the reservoir, based on which efforts are made to acquire information about effective pore and throat radii, effective pore volume per unit of rocks, effective throat radius per unit of volume, ratio of effective pore and throat radii, and sorting coefficient. Further, occurrence characteristics of movable fluids are analyzed from the perspectives of reservoir and seepage capacities. It is demonstrated that movable fluids mainly exist in the macropores, while bound fluids are primarily in the throats and micropores; throat is the main reason for the differences in microscopic heterogeneity; microscopic pore structure is also a key factor influencing occurrence characteristics of movable fluids.

Pore and throat radii, pore–throat radius ratio and sorting coefficient The mercury intrusion experiments of 13 samples in the study area show that the effective pore distribution is uneven and the data points are scattered. The weighted average effective pore radius is mainly distributed between 110 and 192 μm. Generally, smaller pore radius corresponds to poorer reservoir capacity and less occurrence of movable fluids. As for the effective throats, they are fine and tiny, with the weighted average effective throat radius ranging from 0.159 to 0.975 μm. Thus, the weighted average effective pore and throat radius ratio is calculated to range between 174 and 628, with the large values indicating uneven pore–throat distribution and large pore and throat radius difference, which further suggest less effectively connected pores and throats. The sorting coefficient is in the range of 0.06–0.99, indicating good sorting and thus concentrated throat distribution (Table 3).

As can be seen from Fig. 6, the correlation between the movable fluid saturation and the effective pore radius is small, and the correlation coefficient is 0.4627, suggesting unevenly developed, poor pores (Fig. 6a). Comparably, the movable fluid saturation is more correlated with the weighted average effective throat radius with the correlation coefficient of 0.7835 (Fig. 6b). In the throats with radius less than 0.7 μm, movable fluid saturations are all below 50%, while in the throats coarser than 0.7 μm, the movable fluid saturation obviously increases with the weighted average effective throat radius (except for samples 10 and 11). Therefore, it is safe to conclude that throat is the key factor that affects the occurrence characteristics of movable fluids. Larger effective throat radius is favorable for fluids to flow and contributes to larger movable fluid saturation.

With constant pressure mercury intrusion tests, information, such as pore–throat volume ratio and pore–throat radius ratio, can be obtained. It has been demonstrated that pore–throat radius ratio can reflect the pore–throat connectivity and pore–throat coordination relationship. As can be

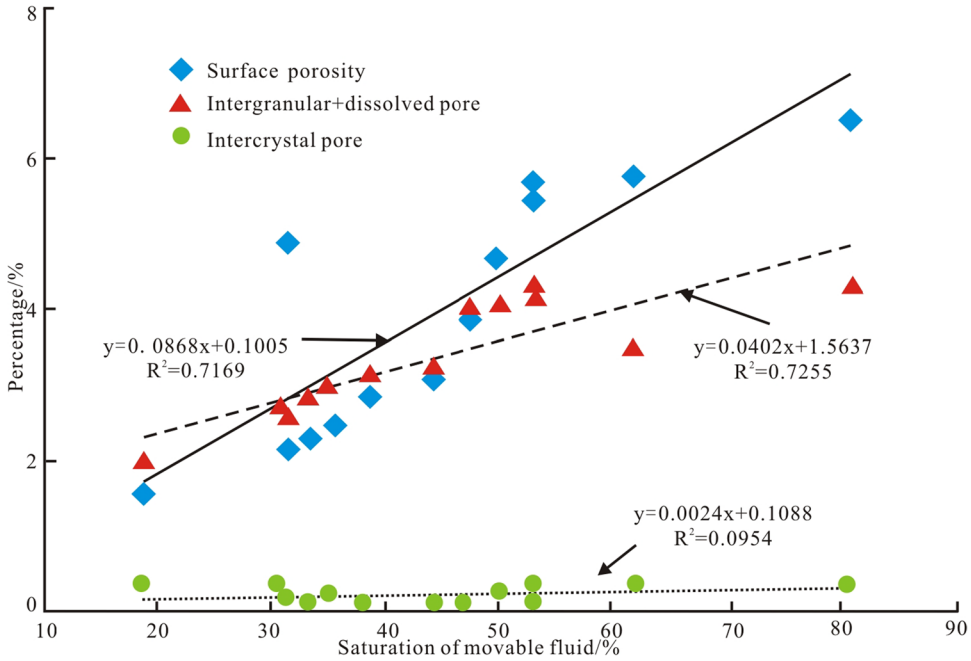

Fig. 5 Relationship between movable fluid saturation and pore types in Chang 8_1 reservoir

Table 3 Characteristic parameters of microscopic pore structures of Chang 8_1 reservoir in Maling Oilfield

Sample ID	Well ID	Total pore mercury saturation (%)	Total throat mercury saturation (%)	Weighted average effective pore radius (μm)	Effective pore volume per unit of rocks (ml/cm^3)	Weighted average effective throat radius (μm)	Effective throat volume per unit of rocks (ml/cm^3)	Weighted average effective pore–throat radius ratio	Sorting coefficient
1	H23	21.556	3.18	191.94	0.082	0.975	0.028	173.514	0.95
2	H56	31.767	8.011	110.893	0.013	0.624	0.003	509.799	0.55
3	L78	34.294	18.316	159.322	0.021	0.486	0.018	594.39	0.06
4	L275-21	38.656	24.773	163.172	0.039	0.505	0.025	577.31	0.37
5	L91	33.855	16.151	155.354	0.078	0.877	0.017	223.15	0.99
6	L98	39.736	21.369	149.672	0.071	0.795	0.029	275.69	0.81
7	L126	23.319	5.375	131.594	0.028	0.522	0.013	526.31	0.41
8	M21	26.44	4.47	110.066	0.027	0.159	0.005	628.234	0.11
9	M23	29.369	4.38	135.204	0.027	0.679	0.015	436.893	0.67
10	M30	8.298	15.967	145.107	0.008	0.852	0.015	319.956	0.89
11	M31	26.461	16.502	158.069	0.059	0.732	0.018	387.809	0.73
12	Y285	33.295	25.366	148.341	0.061	0.651	0.026	486.349	0.62
13	B285	38.841	13.764	149.194	0.067	0.788	0.017	305.162	0.79

seen from Fig. 6, the movable fluid saturation is negatively correlated with the weighted average pore–throat radius ratio, with the correlation coefficient of 0.6988 (Fig. 6c). The pore–throat radius ratio determines the seepage ability of fluids in effective pores. Generally, larger pore–throat radius ratio corresponds to uniform distribution of pores and throats, and thus large pores are blocked by small throats, which increases the seepage resistance and makes it difficult for fluids to flow through. Consequently, the movable fluid saturation is relatively low. However, when the pore–throat radius ratio is small, effective pores are surrounded by large pores and throats, which are favorable for fluid flow and thus contribute to high movable fluid saturation. It should also be noted that as the pore–throat radius ratio decreases, small pores might be surrounded by throats, leading to low movable fluid saturation.

Sorting coefficient also plays a role in controlling the movable fluid saturation. As can be seen in Fig. 6d, there is a good positive correlation between the movable fluid saturation and the sorting coefficient, with a correlation

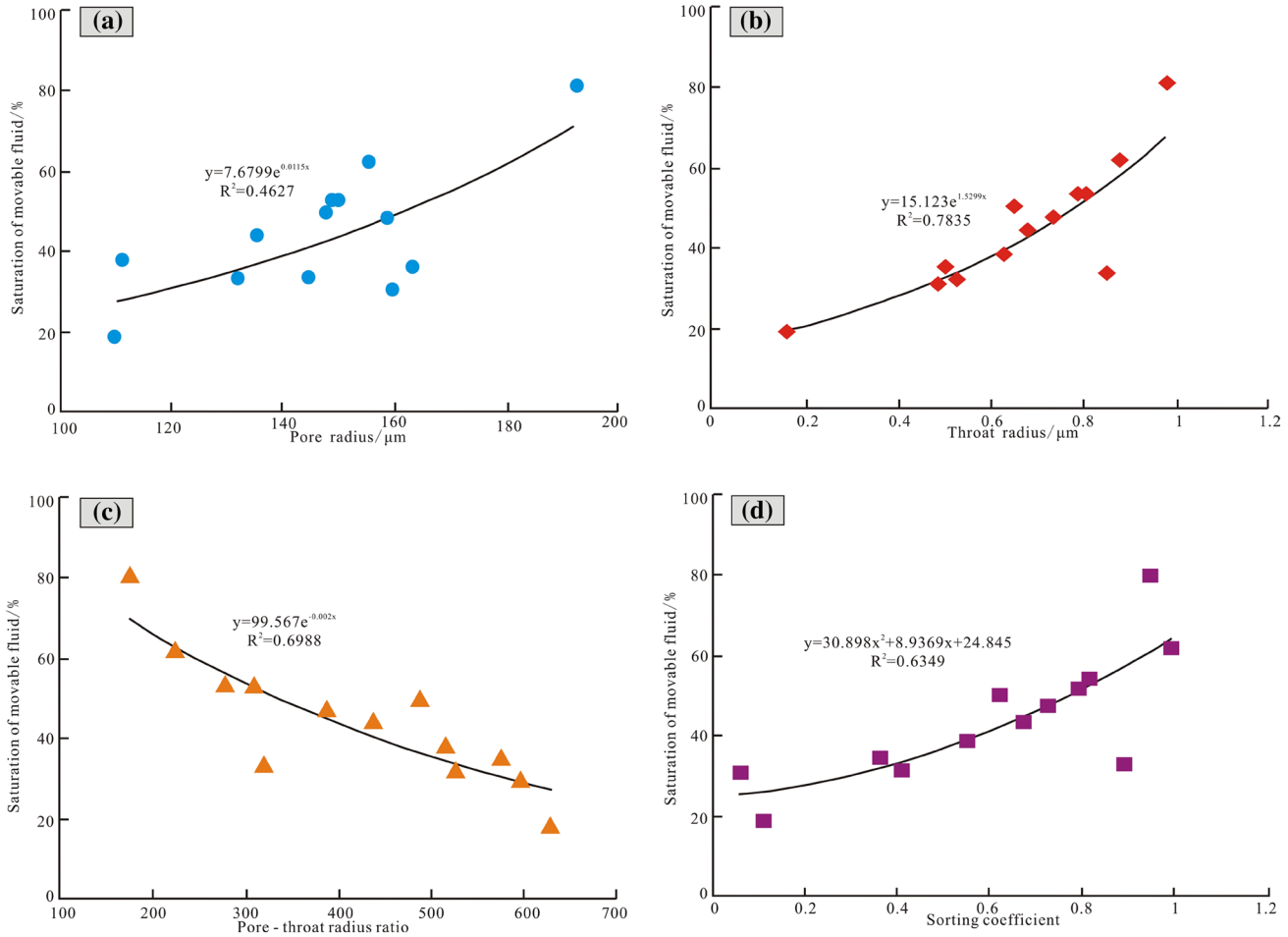

Fig. 6 Relationship between microscopic pore–throat structure parameters and movable fluid saturation in Chang 8_1 reservoir

coefficient of 0.6349. The larger sorting coefficient indicates larger radius and more concentrated distribution of effective throats, which result in better connectivity and higher movable fluid saturation.

Effective pore and throat volumes The reservoir and seepage capacities of fluids in the pores of rocks are commonly influenced by pores and throats. According to the constant pressure mercury intrusion experiments of 13 samples, it is found that there is a good positive correlation between movable fluid saturation and effective pore volume per unit of rocks, with the correlation coefficient of 0.6279 (Fig. 7a), while there is a less positive correlation between movable fluid saturation and effective throat volume per unit of rocks, with the correlation coefficient of 0.3955 (Fig. 7b). Fluids in Chang 8_1 reservoir in the Maling Oilfield mainly occur in the effective pores and throats. Those in the effective pores have stronger seepage capacity, and the movable fluid saturation is more correlated with pore space, while those in the throats suffer poor connectivity and strong bound resistance, making it difficult for fluid to flow.

Based on the above results, it is found that the microscopic pore structure is an important factor affecting the occurrence characteristics of movable fluid saturation. The effective throat radius and the pore–throat radius ratio are the main factors, while the effective pore–throat volume and the sorting coefficient also play relatively important roles.

Clay minerals

The main clay mineral fillings in the Chang 8_1 reservoir of Maling Oilfield are chlorite, illite, kaolinite and illite/smectic mixed layers. The interstitials are mainly in dissolution pores and residual intergranular pores, and some of them are attached to pore-wall surface, seriously destroying the reservoir and influencing the occurrence characteristics of movable fluids.

As observed under the microscope, illite has the highest content (21.36%), followed by chlorite (18.74%), kaolinite (20.05%) and illite/smectic mixed layers (11.38) (Figs. 4, 8). It can be seen from Fig. 8a that the illite content variation

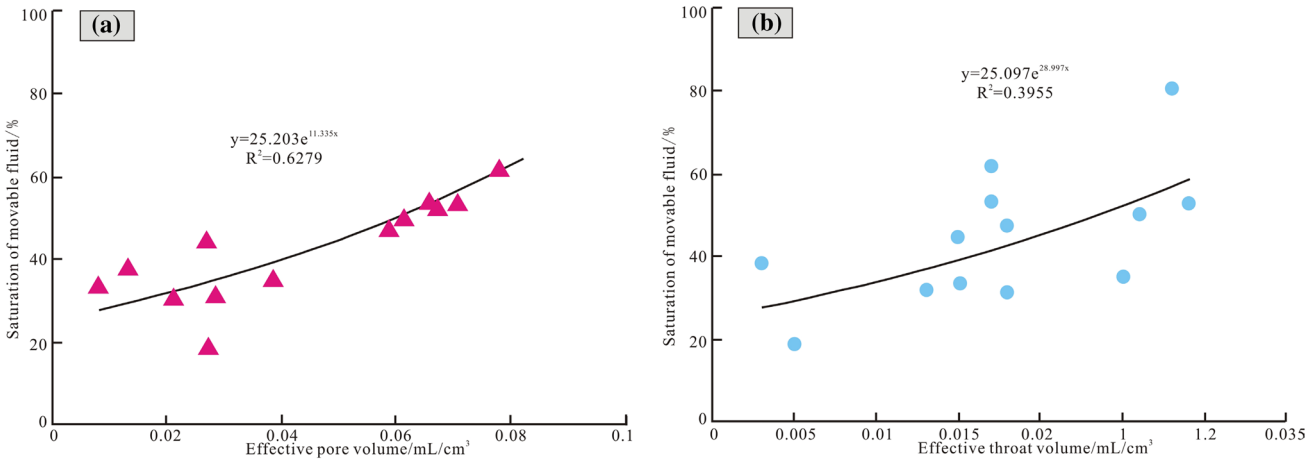

Fig. 7 Relationship between effective pore and throat volumes and movable fluid saturation in Chang 8_1 reservoir

is different in different burial depth intervals, and as shown in Fig. 4c, filamentous and curly features of illites can be observed, and primary pores are isolated and filled due to the illites on the particle surface and in the throats. The relative content of chlorite gradually decreases with the increasing burial depth (Fig. 8b), and chlorite, mainly in the needle-like shape, surrounds the rock particles, leading to the decrease of pore and throat radii and thus resistance for fluids to flow

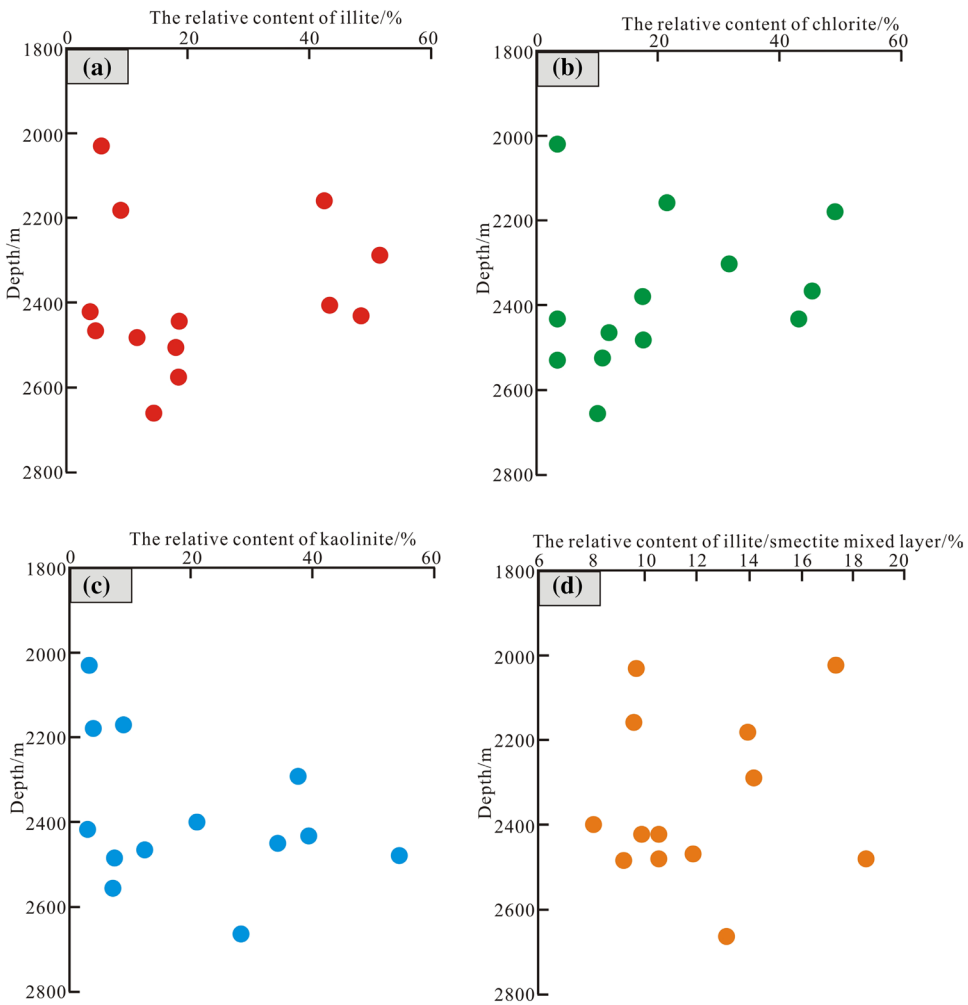

Fig. 8 Relationship between contents of different clay minerals and burial depth in Chang 8_1 reservoir

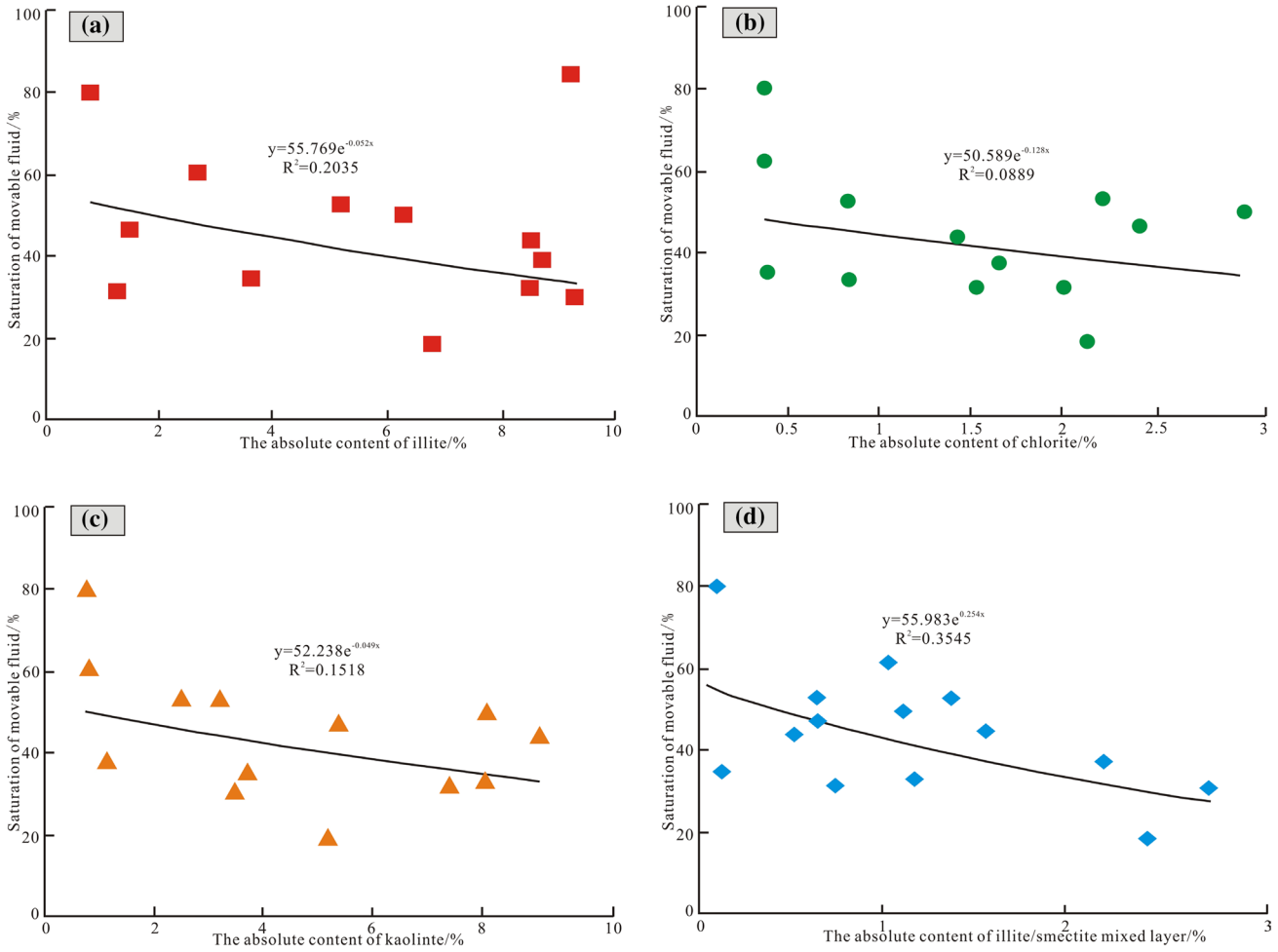

Fig. 9 Relationship between clay mineral contents and movable fluid saturation in Chang 8_1 reservoir

(Fig. 4d). The relative content of kaolinite slightly increases with depth (Fig. 8c), and the book-like kaolinite decreases the intergranular pore space and increases the ineffective pore space though it has rare influence on throats (Fig. 4e). As for the illite/smectic mixed layers, their relative content increases with depth (Fig. 8d), and they are filamentous under the microscope, whose extensive development greatly influences the occurrence of movable fluids (Fig. 4f). It can be seen that clay minerals of different occurrences have different influences on the movable fluid, and more interstitials result in poorer connectivity.

X-ray diffraction analysis shows that the absolute content of clay minerals in Chang 8_1 reservoir ranges from 0.86 to 6.27% with an average of 3.3%. The negative correlations between movable fluid saturation and contents of illite and illite/smectite mixed layer are relatively strong, with respective correlation coefficients of 0.2035 and 0.3545 (Fig. 9a, d), which indicates that their existence can result in poor connectivity and more bound fluids surrounding pores. It is also found that there are very weak negative correlations between movable fluid saturation and chlorite and kaolinite contents with respective correlation coefficients of 0.0889 and 0.1518 (Fig. 9b, c), suggesting their small influence on pores and throats. Therefore, it can be concluded that the content of clay minerals has a certain impact on the occurrence of movable fluids, but such impact originates from the common effect of various clay minerals.

Conclusions

1. The distribution of T_2 spectrum of Chang 8_1 reservoir in the Maling Oilfield, Ordos Basin, is characterized by three kinds of shapes, namely left-high-peak–right-low-peak, left-low-peak–right-high-peak, and unimodal shapes. The movable fluid saturation ranges from 18.85 to 80.59% with an average of 42.06%, which is relatively low. Reservoirs are mainly Class III and Class IV.
2. The main controlling factors that influence the occurrence characteristics of movable fluids are demonstrated

to be reservoir physical property, pore type, pore and throat radii, pore–throat radius ratio, sorting coefficient, effective pore–throat volume, and clay mineral filling.

3. Through analysis of the main controlling factors that influence the occurrence characteristics of movable fluids, it is found that physical properties have certain influence on the movable fluid saturation in the low-permeability reservoir. Specifically, permeability is the main controlling factor with a correlation coefficient of 0.7467, and porosity also plays a role in determining the movable fluid saturation with a correlation coefficient of 0.2424. As for the influence of microscopic pore structure, effective pore and throat radii and pore–throat radius ratio are the primary controlling factors with respective correlation coefficients of 0.7835 and 0.6988, while effective pore radius, effective throat radius, and sorting coefficient also have obvious influence on the movable fluid saturation with respective correlation coefficients of 0.6279, 0.3955, and 0.6349. Meanwhile, clay mineral fillings, pore types and physical properties have relatively small impact. Different clay minerals have different influences on the movable fluid saturation due to their different occurrences, and more interstitials generally lead to poorer connectivity.

References

Al-Mahrooqi SH, Grattoni CA, Muggeridge AH et al (2006) Pore-scale modelling of NMR relaxation for the characterization of wettability. J Pet Sci Eng 52:172–186

Bai R, Li Z, Wang H et al (2016) Fractal nature of microscopic pore throat structure in Chang 7 tight oil reservoir of Longdong area. Sci Technol Eng 16(5):54–59

Cai Y, Liu D, Pan Z et al (2013) Petrophysical characterization of Chinese coal cores with heat treatment by nuclear magnetic resonance. Fuel 108:292–302

Cao L, Sun W, Sheng J et al (2016) A method to determine movable fluid saturation of low-permeability and tight oil reservoirs-by taking tight oil reservoirs in sixth member of Yanchang formation in Banqiao area as an example. J Yangtze Univ (Natural Science Edition) 13(20):1–8 **(in Chinese)**

Chen D, Zhu Y, Zhang J et al (2015) Diagenesis and favorable diagenetic facies of the eight member of Yanchang Formation in Maling area, the Ordos Basin. Petrol Geol Exp 37(6):721–728 **(in Chinese)**

Dai Q, Luo Q, Zhang C et al (2016) Pore structure characteristics of tight-oil sandstone reservoir based on a new parameter measured by NMR experiment: a case study of seventh Member in Yanchang Formation, Ordos Basin. Acta Pet Sin 37(7):887–897

Daigle H, Johnson A (2016) Combing mercury intrusion and nuclear magnetic resonance measurements using percolation theory. Transp Porous Media 111(3):669–679

Dlubac K, Knight R, Song Y et al (2013) Use of NMR logging to obtain estimates of hydraulic conductivity in the High Plains aquifer, Nebraska, USA. Water Resour Res 49(4):1871–1886

Freeman R, Heaton N (2000) Fluid characterization using nuclear magnetic resonance logging. Petrophysics 45(3):241–250

Gao H, Liu YL, Zhang Z et al (2015) Impact of secondary and tertiary floods on microscopic residual oil distribution in medium-to-high permeability cores with NMR technique. Energy Fuel 29(8):4721–4729

Huang H, Ren D, Zhou Y et al (2016) Characteristics of movable fluid and pore evolution of the Chang 8_1 sandstone reservoirs of the Ordos Basin. J Northwest Univ (Natural Science Edition) 46(5):735–745 **(in Chinese)**

Li Y, Fang Y, Deng S et al (2008) Experimental study of pore structure with nuclear magnetic resonance. Prog Explor Geophys 31(2):129–132

Liu D, Sun W, Ren D et al (2016) Features of pore-throat structures and movable fluid in tight gas reservoir: a case from the 8th member of Permian Xiashihezi Formation and the 1st member of Permian Shanxi Formation in the western area of Sulige Gas field, Ordos Basin. Nat Gas Geosci 27(12):2136–2146 **(in Chinese)**

Ma C, Wang R, Luo B et al (2012) Characteristics of Chang 8 oil reservoir and distribution of oil reservoirs in Maling oilfield, Ordos basin. Nat Gas Geosci 23(3):514–519 **(in Chinese)**

Megawati M, Madland MV, Hiorth A (2012) Probing pore characteristics of deformed chalk by NMR relaxation. J Pet Sci Eng 100:123–130

Nelson PH (2009) Pore-throat sizes in sandstones, tight sandstones, and shales. AAPG Bull 93:329–340

Qu X, Sun W, Lei Q et al (2016) Study on saturation of movable fluid in the low-permeability sandstone reservoirs of Huaqing Oilfield and its influencing factors. J Xi'an Shiyou Univ (Natural Science Edition) 31(2):93–98 **(in Chinese)**

Ren X, Li A, Wang Y (2015a) Pore structure of tight sand reservoir and its influence on percolation-taking the Chang 8 reservoir in Maling oilfield in Ordos Basin as an example. Oil Gas Geol 36(5):774–779 **(in Chinese)**

Ren D, Sun W, Lu T et al (2015b) Microscopic geological factors of movable fluid distribution in the tight sandstone gas reservoir: taking the He8 reservoir in the East of Sulige gas field as an example. Geoscience 6:1409–1417 **(in Chinese)**

Ren D, Sun W, Dong F et al (2016a) Characteristics of movable fluids in the Chang 8_1 reservoir, Yanchang formation in Huaqing Oilfield, Ordos Basin and the influencing factors. Geol Explor 27(5):827–834 **(in Chinese)**

Ren Y, Sun W, Ming H et al (2016b) Characteristics of movable fluids in different diagenetic facies and the influencing factors of low-permeability reservoir: taking Chang 6 Jiyuan oilfield as an example. Geoscience 30(5):1124–1133 **(in Chinese)**

Ren Y, Wu K, He K et al (2017) Application of NMR technique to movable fluid of ultra-low permeability and tight reservoir: a case study on the Yanchang formation in Longdong Area, Ordos Basin. J Mineral Petrol 37(1):103–110 **(in Chinese)**

Shi J, Qu X, Lei Q et al (2016) Distribution characteristics and controlling factors of movable fluid in tight oil reservoir: a case study of Chang 7 reservoir in Ordos Basin. Nat Gas Geosci 27(5):827–834 **(in Chinese)**

Wang W, Niu X, Liang X et al (2017) Study on movable fluid saturation in ultra low permeability reservoir: taking Chang 6 reservoir in

Ganguyi oil field as an example. Geol Sci Technol Inf 36(1):183–187 **(in Chinese)**

Wu C, Zhao X, Lu J et al (2017) Determination of T_2 cut-off value of nuclear magnetic resonance in tight sandstone reservoir and lower limit of movable fluid—a case study of Chang 9 reservoir of Wucangbao Oilfield. Unconv Oil Gas 4(2):91–94 **(in Chinese)**

Yan J, Liang Q, Geng B et al (2017) Relationship between micro-pore characteristics and pore structure of low permeability sandstone: a case of the fourth member of Shahejie Formation in southern slope of Dongying Sag. Lithol Reserv 29(3):18–26 **(in Chinese)**

Yang P, Guo H, Yang D (2013) Determination of residue oil saturation during waterflooding in tight oil formations with NMR relaxometry measurements. Energy Fuels 27(10):5750–5756

Yao Y, Liu D (2012) Comparison of low-field NMR and mercury intrusion porosimetry in characterizing pore size distributions of coals. Fuel 95:152–158

Yao JL, Deng XQ, Zhao YD et al (2013) Characteristics of tight oil in Triassic Yanchang Formation, Ordos Basin. Petrol Explor Dev 40(2):161–169

Zhang Y, Pe-Piper G, Piper DJ (2015) How sandstone porosity and permeability vary with diagenetic minerals in the Scotian Basin, offshore eastern Canada: implications for reservoir quality. Mar Pet Geol 63:28–45

Zhao X, Chang B, Zhang J (2016) Distribution of the remaining oil in different flow units for the infill well networks-taken Shuanghe Block, Yanchang Oilfield as an example. Unconv Oil Gas 3(6):60–65 **(in Chinese)**

Zhao X, Dang H, Pang Z et al (2017) Microscopic pore structure and seepage characteristics of different pore assemblage types in ultra-low permeability reservoir: a case of Chang 6 reservoir in Tang 157 well area, Ganguyi Oilfield. Lithol Reserv 29(6):9–14 **(in Chinese)**

Zheng Q, Liu Y (2015) Microscopic pore structure and movable fluid saturation of ultra low permeability reservoir. Geol Sci Technol Inf 34(4):124–131 **(in Chinese)**

Zheng K, Xu H, Chen J et al (2013) Movable fluid study of low permeability reservoir with nuclear magnetic resonance technology. Geoscience 27:710–718 **(in Chinese)**

Zhou Y, Ji Y, Xu L et al (2016) Controls on reservoir heterogeneity of tight sand oil reservoirs in Upper Triassic Yanchang Formation in Longdong Area, southwest Ordos Basin, China: implications for reservoir quality prediction and oil accumulation. Mar Pet Geol 78:110–135

Zou C, Zhu R, Wu S et al (2012) Types, characteristics, genesis and prospects of conventional and unconventional hydrocarbon accumulations: taking tight oil and tight gas in China as an instance. Acta Perolei Sin 33(02):173–187 **(in Chinese)**